

On Numerical Results of a Mathematical Model of Heat Transfer in a Lime Kiln

Amos O. Popoola¹, R.O. Olayiwola² and Ridwan K. Raji¹

¹Department of Mathematical and Physical Sciences, Osun State University, Osogbo, Nigeria.

²Department of Mathematics and Statistics, Federal University of Technology,
P.M.B 65, Minna, Nigeria.

Abstract

The paper studies heat transfer in a lime kiln (a combustion furnace in which a chemical reaction occurs) when the reaction is highly exothermic. We revisit our previous results and investigate for the effects of some sensitive factors on heat transfer under highly exothermic condition.

The paper specifically examines the effects of Frank-Kamenetskii parameter on temperatures of gas and materials, and also study the effect of thermal conductivities on temperatures of gas and materials. A computer program written in C++ language, was used to solve the resulting two-dimensional finite-difference scheme. The results show that Frank-Kamenetskii parameter and scaled thermal conductivity have appreciable effects on temperatures of materials and gas which are favorable in the formation of high quality quick lime. This work therefore establishes the fact that maintaining a high temperature of calcinations increases the furnace productivity.

1.0 Introduction

Before we talk about what have been done in this study, it is necessary to review some basic terms in this theory for better understanding of the process of heat transfer in a lime kiln.. A lime shaft kiln is basically a moving bed reactor with the upward-flow of hot gases passing counter-current to the downward-flow of a feed consisting of limestone particles undergoing calcinations [1].The term calcinations refers to the process of limestone thermal decomposition into quicklime and carbon dioxide. The following chemical reaction takes place in the kiln with dolomitic limestone:



Quick lime is a key industrial mineral used as a chemical additive by many industries. The industrial facilities that utilize lime in various forms are metal ore processing, metallurgy, steel, paper, pharmaceuticals, sulphur removal and water treatment. It is also used for generating many basic chemicals used to manufacture consumer goods.

The rate of conversion of limestone into quicklime depends on the heat of reaction supplied to the limekiln. Heat is created in the kiln by burning pulverized coal, natural gas or oil. Kilns are normally operated at temperatures of 1100°C or higher to drive carbon dioxide from the limestone [1].

Corresponding author: Amos O. Popoola, E-mail: bobdee11@yahoo.com, Tel.: +2348035794352

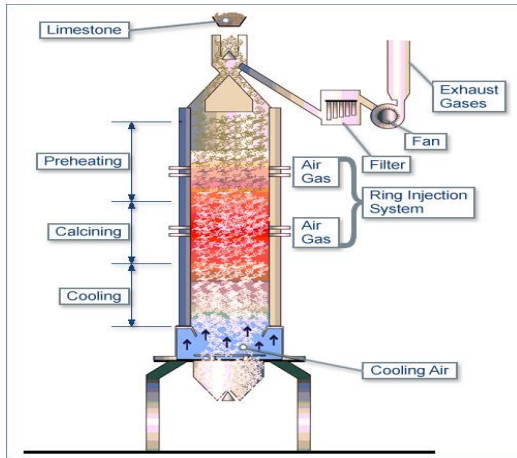


Fig 1.1: Shaft Lime Kiln (Eular [2])

A kiln (See Fig. 1.1) basically has three operating sections: the preheating, the burning and the cooling zone. The preheating zone is that part of the kiln where the limestone is heated to its dissociation temperature. The burning zone is that part of the kiln in which reaction of the burden takes place. The cooling zone is that part of the kiln in which the lime emerging from the burning zone is cooled before discharge. The most common fuels used in shaft kilns are coke, natural gas, weak gas and pulverized lignite. The majority of shaft furnaces for limestone calcination operate with counter-current flows of burden materials and gases. The furnace incorporates three technological zones: preheating, calcination and cooling from (top to bottom).

Numerous heat transfer models for refractory kilns are available in the literature [3 – 8]. The heat transfer model from these previous works has to be solved numerically because of the two dimensional problems which consider the thermal heat conduction in radial and circumferential direction. Heat transfer mechanism is complicated in case of rotary kiln as it includes conduction, convection and radiation together.

The first model for the prediction of the axial transport in a rotary cylinder was proposed by Sullivan in 1927 and then developed to study the isothermal transverse motion of a bed of particulate materials by Friedman and Marshall [9], Peary et al. [10]., Bui and Perron [3].

A mathematical model described by Henein [11] predicted the conditions giving rise to the different forms of transverse bed motion in a rotary cylinder like slumping, rolling, slipping, cascading, contracting, and centrifuging. A 3D steady-state model of a rotary calcimine kiln was also presented by Bui et al. [3] in 1993

Many researchers have different approaches and the available mathematical models are not sound enough to describe the heat transfer between covered kiln wall and the particle in the bed. In general, a rotary kiln can be classified as internally heated and externally heated device. The heat transfer process in rotary kiln is complex; particularly a internally heated kiln.

The majority of shaft furnaces for limestone calcination operate with counter-current flows of burden materials and gases [12 – 15]. The furnace incorporates three technological zones: preheating, calcination and cooling (from top to bottom). Gordon et al. [16] developed the multi-dimensional mathematical model to optimize the furnace design and the process parameters. The developed mathematical model belongs to the group of essentially non-linear models. According to them, it is not possible to develop an analytical solution of the problem. The finite element method was used to provide a solution.

In 2009, Olayiwola et al.[17] developed a mathematical model of calcination process. The developed model took into account the Arrhenius heat generation and chemical reaction. They provided an analytical solution of the model and investigated the effects of activation energy and Frank-Kamenetskii parameters on the gas and material temperatures. In 2013, Olayiwola et al.[1] extended the model developed in [17] to account for a situation where the reaction is not well stirred. They provided an analytical solution of the model and proved the existence and uniqueness of solution of the time-dependent problems. They also examined the properties of solution under certain conditions.

In this paper, following our previous work in Olayiwola et. al[1], we investigated the effects of Frank-Kamenetskii parameters and scaled thermal conductivity on gas and material temperatures. The partial differential equations of the model were solved by finite difference methods.

2.0 Problem Formulation

Following Olayiwola et al.[1], the mathematical model of heat transfer in a lime kiln is given by the equations:

$$\frac{\partial \phi}{\partial t} = \lambda_1 \frac{\partial^2 \phi}{\partial x^2} - \alpha_1 (\theta - \phi) + \beta_1 + \delta_1 \exp \left[\frac{\theta}{1 + \varepsilon \theta} \right] \quad (2.01)$$

$$\frac{\partial \theta}{\partial t} = \lambda_2 \frac{\partial^2 \theta}{\partial x^2} - \alpha_2(\theta - \phi) + \beta_2 + \delta_2 \exp\left[\frac{\theta}{1 + \varepsilon \theta}\right] \tag{2.02}$$

Satisfying;

$$\left. \begin{aligned} \phi(x,0) = 0 & \quad \phi(0,t) = 0 & \quad \phi(1,t) = 0 \\ \theta(x,0) = 0 & \quad \theta(0,t) = 0 & \quad \theta(1,t) = 0 \end{aligned} \right\} \tag{2.03}$$

Nomenclature

Greek symbols	Description
θ	dimensionless temperature for gas
ϕ	dimensionless temperature for material
λ_1	scaled thermal conductivity for material
λ_2	scaled thermal conductivity for gas
δ_1	Frank-Kamenetskii parameter for material
δ_2	Frank-Kamenetskii parameter for gas
β_1, β_2	Scaled Heat sources parameters.
Alphabets	Description
T	Time variable
X	Space variable

In this paper, we provide solutions to the above equations when the reaction is highly exothermic ($\varepsilon \rightarrow 0$). This leads us to the following equations;

$$\frac{\partial \phi}{\partial t} = \lambda_1 \frac{\partial^2 \phi}{\partial x^2} - \alpha_1(\theta - \phi) + \beta_1 + \delta_1 e^\theta \tag{2.04}$$

$$\frac{\partial \theta}{\partial t} = \lambda_2 \frac{\partial^2 \theta}{\partial x^2} - \alpha_2(\theta - \phi) + \beta_2 + \delta_2 e^\theta \tag{2.05}$$

Satisfying;

$$\left. \begin{aligned} \phi(x,0) = 0, \phi(0,t) = 0, \phi(1,t) = 0 \\ \theta(x,0) = 0, \theta(0,t) = 0, \theta(1,t) = 0 \end{aligned} \right\} \tag{2.06}$$

By finite difference method (Thomee [18]), equations (2.04) subject to initial and boundary conditions (2.07) become

$$\phi_{i,j+1} = \frac{\lambda_1 k}{h^2} \phi_{i+1,j} + \frac{\lambda_1 k}{h^2} \phi_{i-1,j} + \left[1 - 2 \frac{\lambda_1 k}{h^2} + k \alpha_1\right] \phi_{i,j} - k \alpha_1 \theta_{i,j} + k \beta_1 + k \delta_1 e^{\theta_{i,j}} \tag{2.07}$$

$$\theta_{i,j+1} = \frac{\lambda_2 k}{h^2} \theta_{i+1,j} + \frac{\lambda_2 k}{h^2} \theta_{i-1,j} + \left[1 - 2 \frac{\lambda_2 k}{h^2} + k \alpha_2\right] \theta_{i,j} - k \alpha_2 \phi_{i,j} + k \beta_2 + k \delta_2 e^{\theta_{i,j}} \tag{2.08}$$

$$\left. \begin{aligned} \phi_{i,0} = 0, \phi_{0,j} = 0, \phi_{1,j} = 0 \\ \theta_{x,0} = 0, \theta_{0,j} = 0, \theta_{1,j} = 0 \end{aligned} \right\} \tag{2.09}$$

where h, k are step lengths for time and space variables respectively.

3.0 Numerical Results

The numerical results obtained from a computer program written in C++ are presented below;

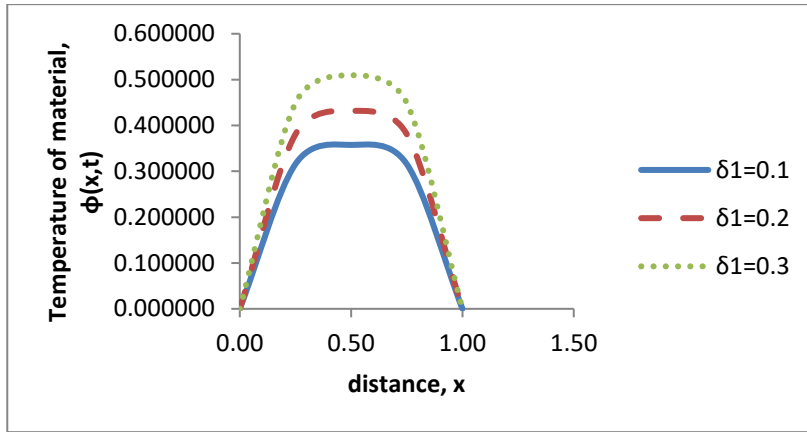


Figure 3.1 : Plot material temperature against distance for different values of δ_1 and for fixed values of $\delta_2 = 0.4, \alpha_1 = 0.3, \alpha_2 = 0.4, \beta_1 = 0.5, \beta_2 = 0.3, \lambda_1 = 0.05, \lambda_2 = 0.2$ at $t = 0.6$

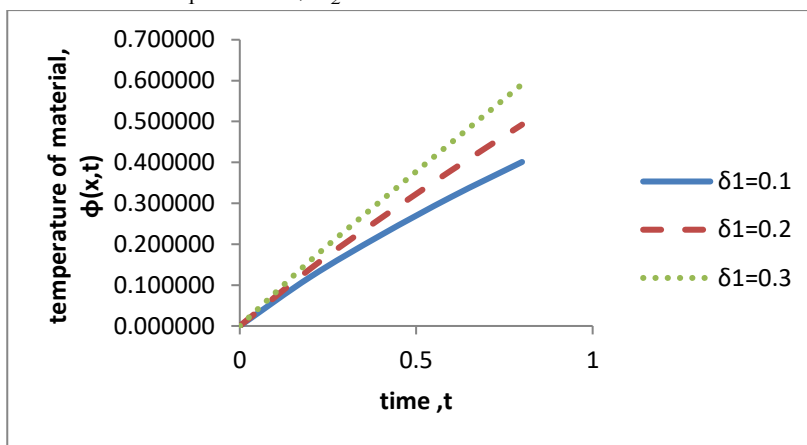


Figure 3.2 : Plot material temperature against time for different values of δ_1 and for fixed values of $\delta_2 = 0.4, \alpha_1 = 0.3, \alpha_2 = 0.4, \beta_1 = 0.5, \beta_2 = 0.3, \lambda_1 = 0.05, \lambda_2 = 0.2$ at $x = 0.25$

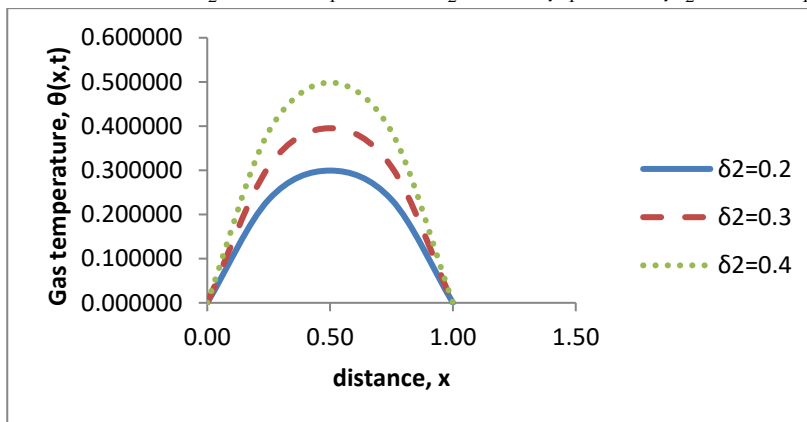


Figure 3.3: Plot gas temperature against distance for different values of δ_2 and for fixed values of $\delta_1 = 0.1, \alpha_1 = 0.4, \alpha_2 = 0.3, \beta_1 = 0.3, \beta_2 = 0.2, \lambda_1 = 0.2, \lambda_2 = 0.1$ at $t = 0.8$

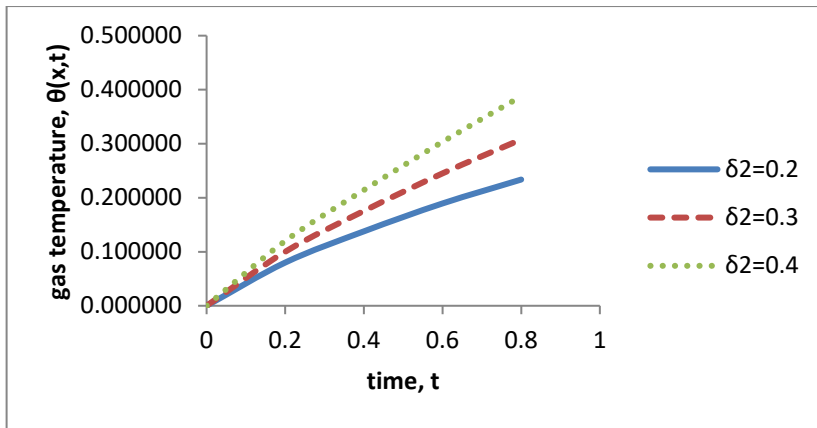


Figure 3.4 :Plot gas temperature against time for different values of δ_2 and for fixed values of $\delta_1 = 0.1, \alpha_1 = 0.4, \alpha_2 = 0.3, \beta_1 = 0.3, \beta_2 = 0.2, \lambda_1 = 0.2, \lambda_2 = 0.1$ at $x = 0.25$

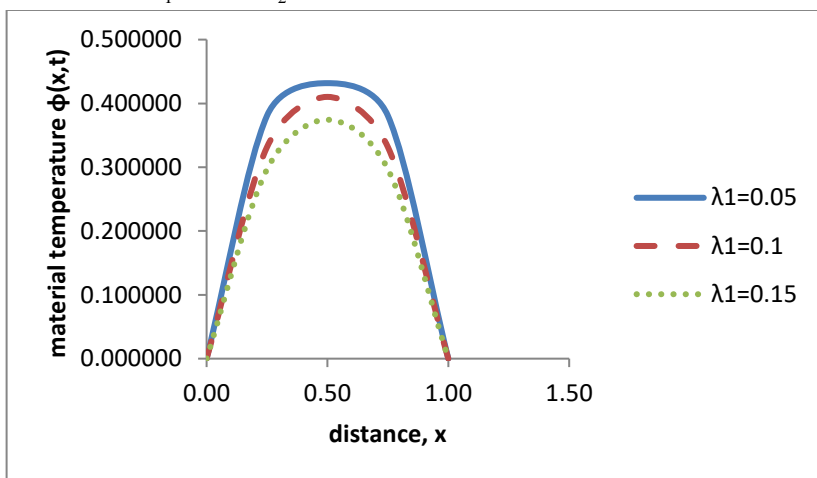


Figure 3.5 :Plot material temperature against distance for different values of λ_1 and for fixed values of $\delta_1 = 0.2, \delta_2 = 0.4, \alpha_1 = 0.3, \alpha_2 = 0.4, \beta_1 = 0.5, \beta_2 = 0.3, \lambda_2 = 0.2$ at $t = 0.6$

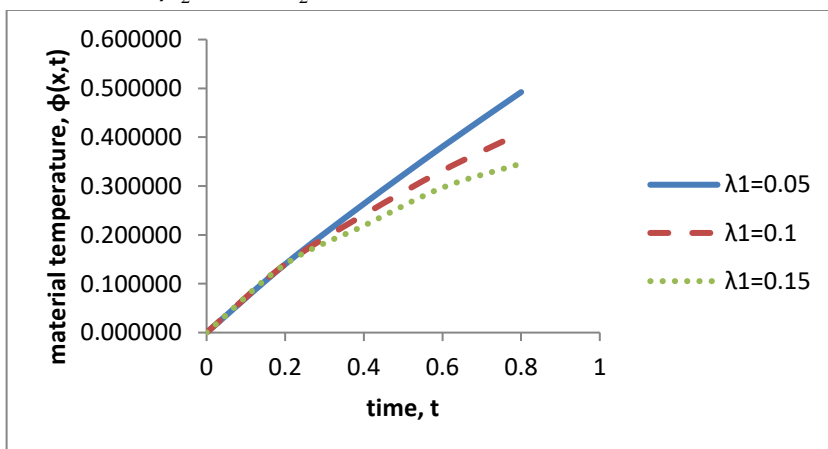


Figure 3.6: Plot material temperature against time for different values of λ_1 and for fixed values of $\delta_1, \alpha_1 = 0.3, \alpha_2 = 0.4, \beta_1 = 0.5, \beta_2 = 0.3, \lambda_2 = 0.2$ at $x = 0.25$

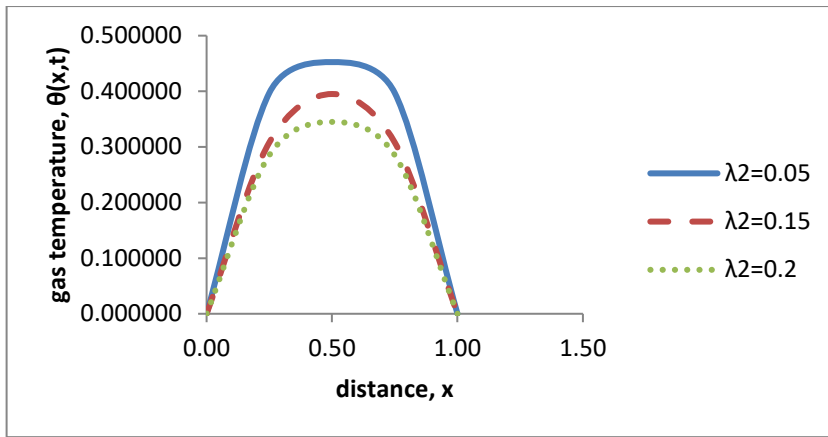


Figure 3.7 : Plot gas temperature against distance for different values of λ_2 and for fixed values of $\delta_1 = 0.2, \delta_2 = 0.4, \alpha_1 = 0.3, \alpha_2 = 0.4, \beta_1 = 0.5, \beta_2 = 0.3, \lambda_1 = 0.1$ at $t = 0.6$

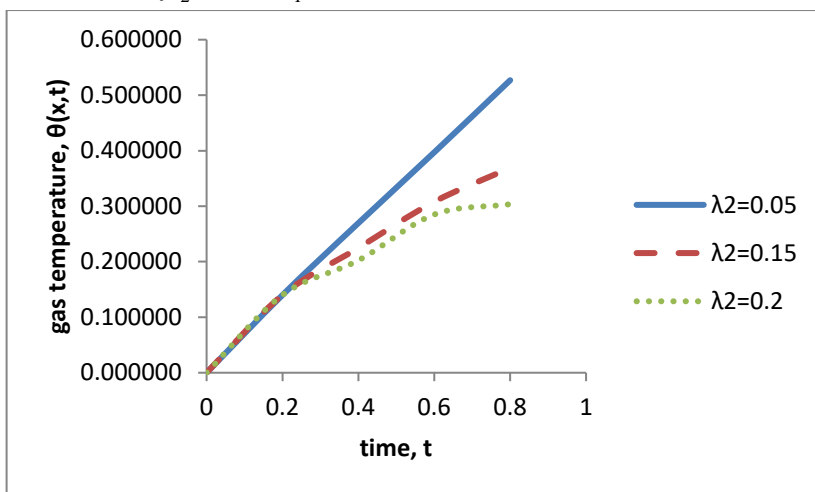


Figure 3.8 : Plot gas temperature against time for different values of λ_2 and for fixed values of $\delta_1 = 0.2, \delta_2 = 0.4, \alpha_1 = 0.3, \alpha_2 = 0.4, \beta_1 = 0.5, \beta_2 = 0.3, \lambda_1 = 0.1$ at $x = 0.25$

4.0 Discussion of Results and Conclusion

The figure 3.1 shows the plot of material temperature ϕ against the position(x). The graph shows that as δ_1 increases, the maximum temperature of material increases. Figure 3.2 shows the plot of material temperature ϕ against time(t). The graph shows that as δ_1 increases, the maximum temperature of material increases. Figure 3.3 shows the plot of gas temperature θ against position(x). The graph shows that as δ_2 increases, the maximum temperature of gas increases. Figure 3.4 shows the plot of gas temperature θ against time(t). The graph shows that as δ_2 increases, the maximum temperature of gas increases. Figure 3.5 shows the plot of material temperature ϕ against the position(x). The graph shows that as λ_1 increases, the maximum temperature of material decreases. Figure 3.6 shows the plot of material temperature ϕ against the time(t). The graph shows that as λ_1 increases, the maximum temperature of material decreases. Figure 3.7 shows the plot of gas temperature θ against the position(x). The graph shows that as λ_2 increases, the maximum temperature of gas decreases. Figure 3.8 shows the plot of gas temperature θ against the time(t). The graph shows that as λ_2 increases, the maximum temperature of gas decreases.

In general, our results showed that as Frank-Kamenetskii parameter increases, the temperature increases with time and with space. The results also showed that as the scale thermal conductivity increases, the temperature of the system lowers with time and space.

In conclusion, the entire results observations have agreed with the practical point of view that scale thermal conductivity and Frank-Kamenetskii parameters have appreciable effects on temperatures of materials and gas even when the reaction is highly exothermic. This also establishes the fact that maintaining a high temperature of calcinations increases the furnace productivity in the formation of high quality quick lime.

5.0 References

- [1.] Olayiwola, R.O., Ph.D; A.O. Adesanya, Ph.D; A.M. Okedoye, Ph.D; and A.O Popoola, Ph.D. (2013) "Lime Shaft Kilns: Modeling and simulation". *The pacific journal of science and technology*, Akama university, USA 14(1):206-215.
- [2.] Eula (2013): Kiln types, <http://www.eula.eu/kiln-types>.
- [3.] Bui R.T., Perron and Read M, (1993) "Mode- based optimization of the operation of the coke calcining kiln", *Carbon*, 31(7): 1139-1147
- [4.] Gardeik, H. O. and Jeschar, R, (1979), "Simplified Mathematical Models for calculating the heat transfer in Internally heated adiabatic rotary kiln (convection models) Part I, Idealized rotary kiln with infinitely large thermal conductivity coefficient of the wall", *Cement lime Gypsum International* , 7 : 201- 210.
- [5.] Gardeike, H. O. and Jeschar, R, (1979), "Simplified Mathematical Models for calculating the heat transfer in internally heated adiabatic rotary kiln (convection models) Part II, Rotating tube with finite value of thermal conductivity of the wall", *Cement lime Gypsum International*. 7: 434-441.
- [6.] Goshdastidar, P. S., Rhodes ,C A ,Orloff, D. I. (1986) Heat transfer in a rotary kiln during incineration of solid waste, *ASME- Papers* 8(85): 1-6.
- [7.] Pearce, K. W. (, 1973),"A Heat transfer model for Rotary kilns", *J. of the Institute of Fuel*, 7: 363- 371.
- [8.] Sass, A., (1967) "Simulation of the Heat transfer phenomenon in a Rotary Kiln, I and EC", *Process Design and Development*, 6 (4):532-535.
- [9.] Freidman S. J, Marshall W R. J. (1949)," Studies in Rotary drying, Part II. Heat and Mass transfer", *Chemical Engineering Progress*, 45(9): 573,
- [10.] Peary, K. E., Waddell, J.J. (1972), *The rotary cement kiln*, Chemical publishing co., New York.
- [11.] H. Henein., (1980), "Bed behaviour in Rotary Cylinders with Applications to Rotary Kilns". PhD Dissertation, University of British Columbia, Vancouver,
- [12.] Boynton, R.S. (1980). *Chemistry and technology of lime and limestone*. John Wiley and sons, Inc.: New York, NY.

- [13.] Terruzzi, D. (1994). "Lime Shaft Kilns Using Two Way Pressure System". ZKG International. 6:322-326.
- [14.] Tabunshikov, N.P. (1974). Lime Production, Chemistry Publishing House, Moscow, Russia.
- [15.] Monastirev, A.V and A.V Aleksandrov (1979) Furnace for Lime Production. Metallurgy: Moscow Russia.
- [16.] Gordon, Y.M., M.E. Blank, V.V Madison, and P.R. Abovian. (2003). "New Technology and shaft Furnance for High Quality Metallurgical Lime Production". Proc. Of Asia Steel International Conference, Jamshedpur, India. 9- 12.
- [17.] Olayiwola, R.O., A.T. Cole, D. Hakimi, and R.O. Ayeni. (2009). "Mathematical Modelling of the Calcination Process". J. Nig. Assoc. of Math/phys. 14(1):381 -388..
- [18.] Vidar Thomee. (1999). "From finite differences to finite elements, a short history of numerical analysis of partial differential equations". Journal of Computational and Applied Mathematics 128 (2001) 1–54